

## INFLUENCE OF Tb CONCENTRATION ON CHARGE CARRIER KINETICS AND STRUCTURAL DEFECTS IN $Tb_xSn_{1-x}Se$ ALLOYS

T.A. JAFAROV<sup>1</sup>, O.M. GASANOV<sup>1</sup>, Kh.A. ADGEZALOVA<sup>1</sup>, H.A. ASLANOV<sup>1</sup>,  
J.I. HUSEYNOV<sup>1</sup>, I.I. ABBASOV<sup>2</sup>

<sup>1</sup>*Azerbaijan State Pedagogical University  
AZ-1000, Baku, Uz.Hajibeyli Str.68, Azerbaijan  
[xatirafizik@mail.ru](mailto:xatirafizik@mail.ru);*

<sup>2</sup>*Azerbaijan State Oil and Industry University  
Az-1010, Baku, Azadliq Avenue 20, Azerbaijan*

The structural and kinetic properties of  $Tb_xSn_{1-x}Se$  ( $0 \leq x \leq 0.05$ ) alloys grown by the Bridgman method were investigated. X-ray analysis showed that solid solutions are formed in accordance with Vegard's law, with lattice parameters increasing with Tb concentration. Electrical measurements revealed that pure SnSe exhibits p-type conductivity, while at  $x \approx 0.25$  mol% a transition from p-type to n-type conductivity occurs. With increasing Tb content, the electron concentration rises, the Hall coefficient stabilizes at negative values, and mobility remains nearly constant due to the formation of defect complexes. The results confirm the crucial role of Tb doping in controlling the electronic properties of SnSe-based solid solutions.

**Keywords:** solid solution, electrical conductivity, Hall coefficient, cation vacancy, conductivity type transition, charge carrier mobility, crystal lattice defects, rare-earth dopant impurities.

**DOI:**10.70784/azip.1.2025332

### 1. INTRODUCTION

Semiconductor materials form the basis of modern electronics and energy-intensive technologies. In recent years, particular attention has been drawn to binary semiconductors of the  $A^{IV}B^{VI}$  type, which possess excellent thermoelectric and optoelectronic properties. These compounds, comprising group IV elements (*Sn, Ge*) and group VI elements (*S, Se*)—such as *SnS, SnSe, GeS, and GeSe*—generally exhibit orthorhombic or monoclinic crystal structures with a characteristic layered organization. The weak van der Waals interactions between layers give rise to anisotropic physical properties, which are manifested in differing electrical and thermal conductivities along various crystallographic directions [1, 2].

Materials with a narrow band gap absorb light efficiently, making them promising candidates for use in photovoltaic converters, solar cells, and photodetectors. Their low thermal conductivity (around  $0.5\text{--}1.0\text{ W}/(m \cdot K)$ ) enhances their performance in thermoelectric devices, where the figure of merit (*ZT*) can reach up to 2.6. This is particularly relevant for *SnSe*, which is well-suited for thermoelectric generators and systems for converting heat into electrical energy. The laminar structure of these materials also facilitates the fabrication of thin films and nanostructures [3, 4].

The constituent elements (*Sn, Ge, Se, S*) are relatively inexpensive and environmentally friendly. The physical properties of these materials can be widely tuned through doping and elemental substitution. Doping with rare-earth metals such as terbium (*Tb*) alters the crystal lattice, creates localized energy levels, affects the concentration and mobility of charge carriers, and enhances phonon

scattering, thereby reducing thermal conductivity and increasing thermoelectric efficiency. Rare-earth elements also influence optical and magnetic properties, expanding potential applications in optoelectronics and spintronics [5–7].

In the present study, the influence of terbium content on the galvanomagnetic properties of solid solutions  $Tb_xSn_{1-x}Se$  based on the binary compound *SnSe* is investigated.

### 2. EXPERIMENTAL METHODOLOGY

For the synthesis of alloys  $Tb_xSn_{1-x}Se$ , tin of grade "B4-000", selenium "OC417-4", and pure terbium (99.98%) were used. The synthesis was carried out in vacuum-sealed quartz ampoules (pressure  $0.1333\text{ Pa}$ ) by a two-step direct melting method: first, the mixture was heated to the melting temperature of selenium and held for 3–4 hours, then the temperature was increased to  $950\text{--}1000\text{ }^\circ\text{C}$  and held for 8–9 hours [8].

The interaction in the *SnSe–TbSe* system was studied by differential thermal analysis (DTA), X-ray phase analysis (XPA), microstructural analysis (MSA), microhardness and density measurements. DTA was performed on a PerkinElmer STA 6000 instrument at a heating rate of  $5\text{ }^\circ\text{C}/\text{min}$  in nitrogen atmosphere ( $20\text{ ml/s}$ ). X-ray structural analysis was conducted using a Rigaku Miniflex diffractometer ( $CuK\alpha$ ,  $30\text{ kV}$ ,  $10\text{ mA}$ ,  $2\theta = 0\text{--}80^\circ$ ). Morphology and microcomposition were studied by scanning electron microscopy (SEM) using a JEOL JSM6610-LV microscope. Electrical conductivity and Hall coefficient were measured under constant current and magnetic field with an error margin of no more than 4.2% [9].

**3. RESULTS AND DISCUSSION**

The thermograms of the alloys in the  $Tb_xSn_{1-x}Se$  system show sharp peaks during heating and cooling, which correspond to the melting and solidification temperatures, indicating the formation of congruently melting alloys. In the SnSe compound, partial substitution of Sn with Tb lowers the melting temperature due to the incorporation of larger rare-earth (RE) ions, which cause distortion of the crystal lattice and weakening of interatomic bonds. This leads to structural defects and an additional decrease in melting temperature. The microhardness of samples with TbSe content up to 0.05 mol. % remains at the level of ~500 MPa.

Analysis of the intensity of X-ray reflections shows that the sample has a preferred crystal orientation and consists of a single phase. Indexing of the X-ray patterns indicates an orthorhombic crystal system with the space group  $D_{2h}^{16} - Pcmn$  (Fig. 1). In

the range  $0 \leq x \leq 0.05$ , no shift in diffraction lines is observed; only their intensity changes, which indicates the formation of solid solutions based on SnSe. When Sn atoms are partially replaced with RE atoms of larger ionic radius, the intensity of reflections decreases, and the lattice parameters increase additively. The increase in parameters is linear, with no deviations from Vegard's law observed.

X-ray structural analysis shows that the addition of gadolinium selenides leads to an increase in the unit cell parameters of SnSe as the concentration of Tb increases. This is accompanied by intense scattering of charge carriers due to lattice distortion, which is consistent with the low thermal conductivity of the alloys [11]. At the same time, the density of the  $Tb_xSn_{1-x}Se$  system remains practically unchanged, indicating interstitial positioning of Tb atoms and the formation of Frenkel-type defects [12].

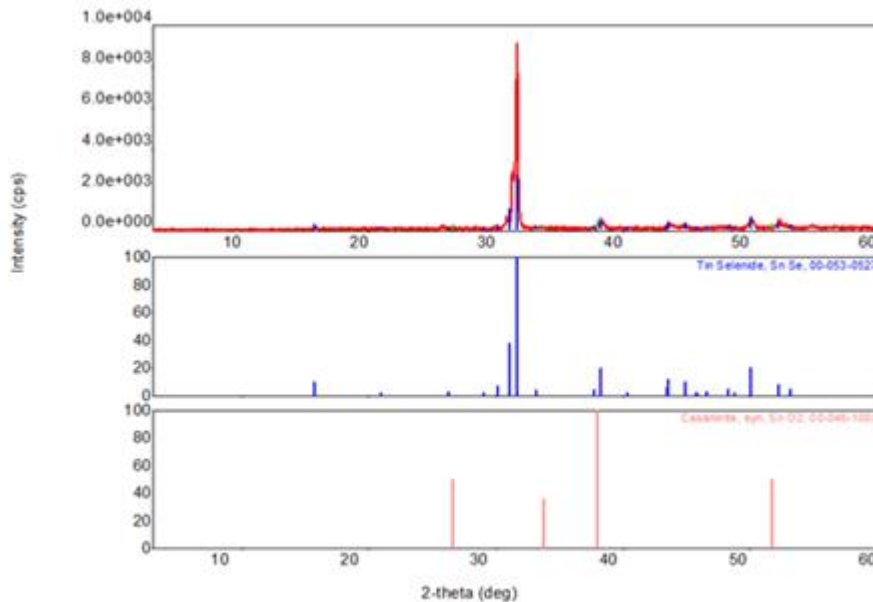


Fig. 1. X-ray diffraction spectrum of crystals  $Tb_xSn_{1-x}Se$  : $x=0,0025$ . Below are X-ray diffraction patterns of SnSe and SnO for comparison.

The increase in lattice parameters, the coherent substitution of Sn with Tb, and adherence to Vegard's law confirm the formation of a substitutional solid solution based on SnSe. X-ray structural analysis and pycnometry revealed that the solubility range of TbSe in SnSe at room temperature is limited to 2 mol. %.

Comprehensive physicochemical analysis showed that the  $Tb_xSn_{1-x}Se$  system alloys, like SnSe, crystallize in an orthorhombic crystal system. With an increase in TbSe content, the lattice parameters, density, and microhardness increase slightly, while the thermal effects shift to lower temperatures. Due to differences in the electronic configuration of Sn and Tb, substitution in the  $Tb_xSn_{1-x}Se$  solid solution

leads to distortions in the SnSe crystal lattice, while preserving its basic structure.

Atomic force microscopy of the surface topography of  $Tb_xSn_{1-x}Se$  crystals revealed that the natural surface is inhomogeneous and has a roughness of about 25 nm. This is due to the presence of weak van der Waals forces between the layers, which lead to the formation of atomic clusters upon cleavage, giving the surface an uneven appearance. X-ray microanalysis revealed the phase composition and element distribution (Fig. 2). The surface was generally homogeneous; however, an excess of selenium was observed within the homogeneity range of SnSe.

In the solid solution region at  $0 \leq x \leq 0.05$ , some kinetic parameters were studied at room

temperature (300 K) for samples containing *TbSe* grown by the Bridgman method: specific electrical conductivity ( $\sigma$ ), Hall coefficient ( $R$ ), charge carrier concentration ( $p, n$ ), and Hall mobility ( $\mu$ ). The obtained values are presented in Table 1.

The *SnSe* compound, in the absence of doping impurities, consistently exhibits *p*-type conductivity, which has been confirmed both by experimental measurements and quantum-chemical calculations [13, 14]. The primary reason for this is the presence of intrinsic defects in the crystal lattice — primarily tin cation vacancies ( $V_{Sn}$ ), which act as acceptor centers and promote hole generation.

The formation of such vacancies can be explained based on the atomic properties and electronic structure of the *SnSe* components. Firstly, tin (*Sn*) is characterized by a relatively low ionization energy (the first ionization energy is approximately 7.34 eV [8]), which facilitates the loss of valence electrons and promotes the transition of tin atoms to the ionic state  $Sn^{2+}$ . Secondly, selenium (*Se*), possessing a high electronegativity (2.55 on the Pauling scale [14]), strongly attracts electrons from the covalent *Sn-Se* bond, thereby further polarizing and weakening this bond. This makes tin cations less stable in the lattice, especially under synthesis conditions with excess selenium, and contributes to the formation of cation vacancies.

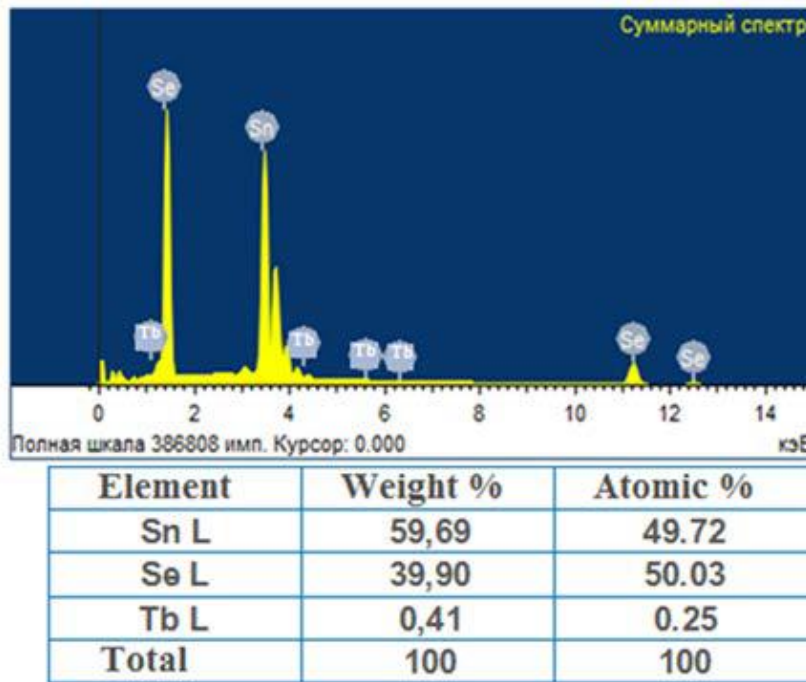


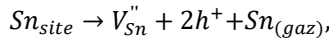
Fig. 2. X-ray microanalysis of the crystal surface  $Tb_xSn_{1-x}Se$  ( $x=0,005$ ).

Table 1.

Some kinetic parameters of  $Tb_xSn_{1-x}Se$  alloys at  $T = 300$  K

Composition, $x, \text{mol}\%$	$R, \text{cm}^2/\text{K}$	$\sigma, \Omega^{-1} \cdot \text{cm}^{-1}$	$\mu, \text{cm}^2/\text{V} \cdot \text{sec}$	$p(n) \times 10^{17}, \text{cm}^{-3}$
0,00	+8,68	18	156	7,2
0,10	+25,7	2,42	60,5	2,43
0,20	+32,3	0,45	14,5	1,93
0,25	-180	0,027	4,86	0,347
0,50	-1750	0,012	21,12	0,036
1,00	-1260	0,0063	6,50	0,05
1,5	-1040	0,0061	6,34	0,06
2,00	-898	0,006	5,39	0,07
2,5	-420	0,012	5,04	0,15
3,00	-245	0,028	6,86	0,26
3,5	-176	0,035	6,16	0,36
4,00	-70	0,04	2,82	0,89
4,5	-54	0,043	2,3	1,16
5,00	-41,6	0,047	3	1,5

According to modern concepts of defect thermodynamics, under thermodynamic equilibrium conditions in *SnSe*, the reaction of cation vacancy formation can be described by the equation:



where  $V_{Sn}''$  – is a tin cation vacancy with a double negative charge, and  $h^+$  – is a hole (positive charge carrier) [3]. This type of defect is thermodynamically stable when the stoichiometry is not strictly maintained, especially with a slight tin deficiency. These holes can move freely, providing hole (*p*–type) conductivity. Thus, the formation of vacancies is accompanied by an increase in the hole concentration, which determines the *p*–type conductivity.

Results from DFT calculations confirm that the formation energy of tin cation vacancies is significantly lower than that of other possible intrinsic defects (such as selenium vacancies or antisite defects), especially under *Se*–rich conditions [13, 16]. This indicates the thermodynamic preference for the formation of such defects corresponding to *p*-type conductivity.

At low *Tb* content, the Hall coefficient is positive, indicating the predominance of hole conductivity. The increase of  $R_H$  from +8.68 to +32.3  $cm^3/C$  indicates a decrease in carrier concentration and the possible formation of acceptor levels due to the introduction of  $Tb^{3+}$ , which substitutes for  $Sn^{2+}$ . The sharp change in sign from positive to negative at 0.25 *mol%* *Tb* reflects an inversion of the conductivity type from hole to electron. This may be caused either by a transition from acceptor to donor behavior of *Tb* or by a change in the material's band structure, whereby levels are formed that efficiently generate electrons.

At the conductivity type inversion point (where the transition from hole to electron conduction occurs), the Hall coefficient  $R_H$  is determined by the two-carrier model, since in this region both electrons and holes are present simultaneously and their contributions compete. The generalized formula for the Hall coefficient in the presence of two types of carriers is:

$$R_H = \frac{p\mu_p^2 - n\mu_n^2}{e(p\mu_p + n\mu_n)^2}$$

where *p*– is the hole concentration, *n*– is the electron concentration,  $\mu_n$ – and  $\mu_p$ – are the mobilities of electrons and holes respectively, and *e* is the elementary charge [17]. At the inversion point, the condition  $p\mu_p^2 = n\mu_n^2$  holds and the Hall coefficient becomes  $R_H = 0$ . When  $\mu_p^2 < n\mu_n^2$ , the sign of  $R_H$  becomes negative, indicating electron dominance.

The change of sign and sharp increase in the magnitude of the Hall coefficient at  $x = 0.0025$  (0.25 *mol%*) in the  $Tb_xSn_{1-x}Se$  system is a

key transitional point in the electronic structure of the material. The abrupt change of sign to negative indicates a transition to electronic (*n*–type) conductivity. This means that *Tb* begins to act effectively as a donor, introducing electrons into the conduction band [18].

After the sharp jump in  $R_H$  at  $x = 0.0025$ , further addition of *Tb* leads to an increase in electron concentration, since *Tb* continues to function as a donor. However, the Hall coefficient is inversely proportional to the carrier concentration. That is, the higher the carrier concentration, the smaller the magnitude of the Hall coefficient, even if the carriers remain of electronic type [19].

In the composition range  $0.03 < x < 0.05$ , a noticeable stabilization of the Hall coefficient value is observed, which remains at a relatively low negative level, close to  $-50 cm^3/C$ . This phenomenon indicates that a certain electronic equilibrium is reached in the material at this terbium concentration. It reflects the formation of a stable electronic structural configuration, which is an important factor for predicting and controlling the electronic properties of these alloys at high rare-earth dopant concentrations.

The graph of the dependence of the free charge carrier concentration on the atomic percentage of *Tb* in the composition of  $Tb_xSn_{1-x}Se$  system alloys at room temperature is shown in Figure 3. In the binary compound *SnSe*, *Sn* atoms (cations) are partially substituted by *Tb* atoms. Since *Tb* and *Sn* have different electronic configurations and valence states, this substitution leads to changes in the concentration of donor or acceptor states in the crystal. In pure *SnSe*, the carrier concentration (*p*(*n*)) is relatively high ( $\sim 7.2 \cdot 10^{17} cm^{-3}$ ). Upon the introduction of a small amount of *Tb*, the carrier concentration sharply decreases, reaching a minimum at approximately 0.5 *mol%* *Tb*. This can be attributed to the fact that *Tb* atoms compensate existing defects or create new localized states that trap free carriers, thereby reducing their concentration [20].

*Tb* atoms may form defect complexes with *Sn* or *Se* vacancies, altering the balance of donors and acceptors. At low *Tb* concentrations, defects responsible for free carriers may be compensated, leading to a sharp decrease in carrier concentration. With a further increase in *Tb* content (beyond the concentration minimum), a rise in carrier concentration is observed. This may be explained by the formation of new donor levels at higher *Tb* concentrations, which begin to dominate, or by the onset of self-doping, which increases the carrier concentration [21].

Partial substitution of *Sn* cations by *Tb* in *SnSe* results in complex changes in the free carrier concentration due to defect compensation, modification of the electronic structure, and the formation of new donor or acceptor centers. This explains the observed nonlinear behavior of the carrier concentration with increasing *Tb* content.

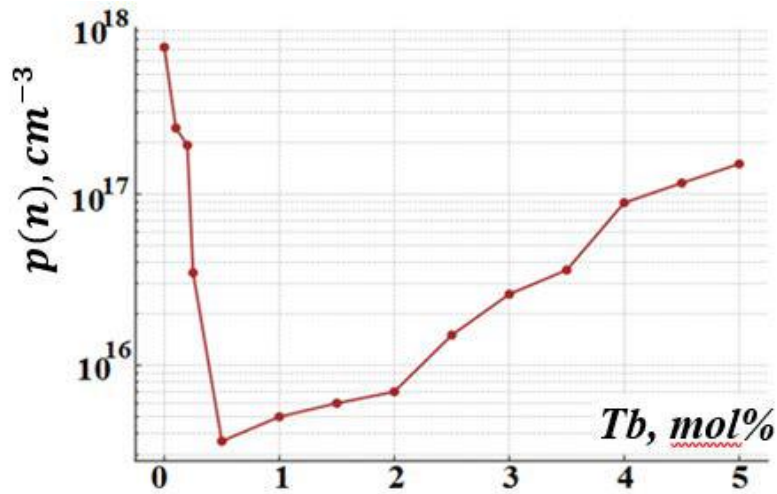


Fig. 3. Composition dependence of charge carrier concentration in  $\text{Tb}_x\text{Sn}_{1-x}\text{Se}$  system alloys

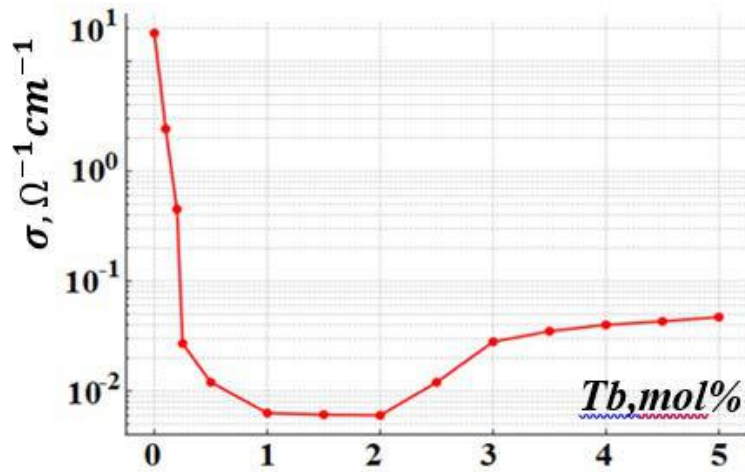


Fig. 4. Composition dependence of specific electrical conductivity in  $\text{Tb}_x\text{Sn}_{1-x}\text{Se}$  system alloys.

Based on the experimental data, it has been established that the electrical conductivity ( $\sigma$ ) of the  $\text{Tb}_x\text{Sn}_{1-x}\text{Se}$  system exhibits a pronounced nonlinear dependence on the terbium content (Figure 4). As the concentration of  $\text{Tb}$  increases from 0 to 2 mol%, there is a sharp drop in electrical conductivity by more than three orders of magnitude — from  $18 \Omega^{-1} \cdot \text{cm}^{-1}$  to  $0.006 \Omega^{-1} \cdot \text{cm}^{-1}$ . The substitution of  $\text{Sn}$  atoms by  $\text{Tb}$  may alter the concentration of free charge carriers, since  $\text{Tb}$  can have a different charge or valence state compared to  $\text{Sn}$ . This affects the carrier balance, which in turn influences conductivity and mobility [22].

At the initial stage of doping ( $x \leq 0.02$ ), the substitution of  $\text{Sn}^{2+}$  ions by  $\text{Tb}^{3+}$  ions causes significant disruption of the crystal lattice, which leads to an increased concentration of structural defects and charge carrier traps. These defects promote electron localization, reduce carrier mobility, and decrease the effective concentration of free carriers, collectively leading to a drop in electrical conductivity. Moreover, the possible formation of  $\text{Tb}$  –induced energy levels

within the band gap may further enhance carrier localization and increase the activation energy of conductivity.

Starting from a concentration of approximately 2.5 mol% and higher, the electrical conductivity begins to increase. This may indicate the emergence of new charge transport mechanisms. In particular, the formation of  $\text{Tb}$  –rich phases or cluster structures with their own conductivity is possible, or conductivity may occur via hopping of carriers between localized states (variable-range hopping mechanism). An additional contributing factor might be the reduction of lattice defects due to the stabilization of  $\text{Tb}$  atoms in specific positions within the structure.

Thus, the observed dependence of  $\sigma(x)$  in the  $\text{Tb}_x\text{Sn}_{1-x}\text{Se}$  system reflects the complex interplay between the defect structure, energy spectrum, and charge transport mechanisms, which is characteristic of semiconductors doped with rare-earth elements [23].

Figure 3 shows the graph of the dependence of charge carrier mobility in the  $Tb_xSn_{1-x}Se$  alloy system on the atomic percentage of  $Tb$  in the composition at room temperature. The variation in the Hall mobility of charge carriers ( $\mu$ ) in the  $Tb_xSn_{1-x}Se$  system at room temperature is associated with effects arising from the substitution of Sn atoms by  $Tb$  atoms in the cation sublattice. When  $Tb$  atoms are introduced into the  $SnSe$  structure, a partial substitution of Sn atoms by heavier and ionized  $Tb$  atoms occurs. These impurity atoms create local distortions in the crystal lattice and potential fields that enhance the scattering of charge carriers (electrons or holes). The increased scattering leads to a reduction in mobility [24].

As seen in Figure 5, at low  $Tb$  concentrations (up to 0.25 mol%), there is a sharp decrease in  $\mu$ . This is due to the fact that the addition of impurity Tb atoms sharply increases the number of point defects. Even a small amount of impurities significantly disturbs the crystal, creating active scattering centers that strongly

scatter charge carriers, resulting in a marked reduction in mobility.

With a further increase in concentration, the number of defects ceases to be critical, and the additional introduction of impurity atoms has a lesser effect — the system becomes "saturated" with defects [25]. At high  $Tb$  concentrations, the formation of a more homogeneous structural configuration may begin — for example, defect complexes, localized regions with a uniform distribution of  $Tb$ , or even a new quasi-stable phase may form.

Such structural adaptation reduces the level of local distortions and prevents a further sharp increase in carrier scattering, thereby stabilizing mobility. After reaching a certain threshold concentration of  $Tb$ , the system undergoes restructuring; defects and lattice distortions become more organized and "stable", the carrier scattering stabilizes, and as a result, the carrier mobility ceases to decrease sharply and reaches a more stable level.

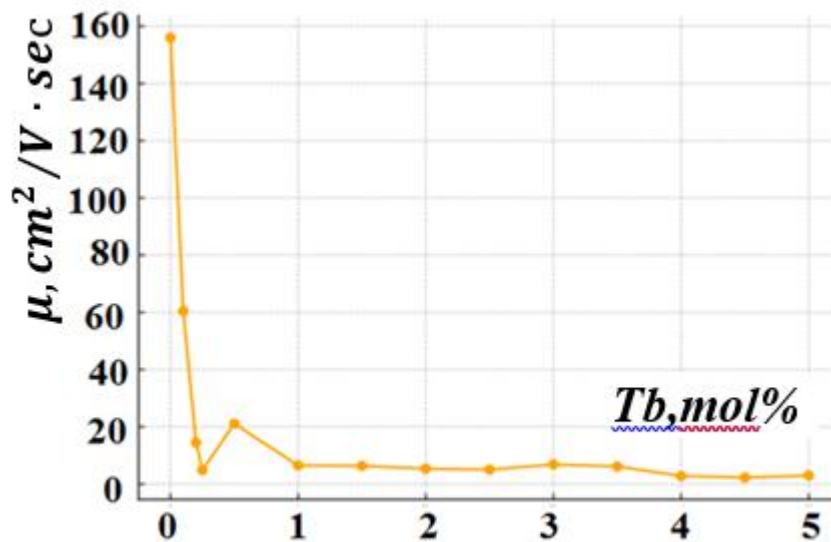


Fig. 5. Composition dependence of charge carrier mobility in  $Tb_xSn_{1-x}Se$  system alloys.

## CONCLUSIONS

In the region of solid solutions  $Tb_xSn_{1-x}Se$  with low concentrations of terbium ( $0 \leq x \leq 0.05$ ), a complex dependence of kinetic parameters—such as electrical conductivity, Hall coefficient, charge carrier concentration, and Hall mobility—on the  $Tb$  content has been revealed. In pure  $SnSe$ ,  $p$ -type conductivity is observed, which is attributed to tin cation vacancies acting as acceptor centers.

The introduction of  $Tb^{3+}$  leads to a reduction in hole concentration at low terbium levels, reflected in an increase in the positive Hall coefficient and a decrease in electrical conductivity by more than three orders of magnitude. At a  $Tb$  concentration of approximately 0.25 mol%, a conductivity type inversion from  $p$ -type to  $n$ -type occurs. This is associated with the transition of  $Tb$  from acceptor to

donor behavior and a change in the electronic structure of the material.

With further increases in  $Tb$  content, an increase in electron concentration and stabilization of the Hall coefficient at a negative value are observed, indicating the formation of a stable electronic structure with donor-type  $Tb$  centers. The charge carrier mobility drops sharply at low  $Tb$  concentrations due to an increase in the number of point defects and enhanced scattering. However, at higher concentrations, mobility stabilizes as a result of the formation of defect complexes and structural adaptation.

These results highlight the key role of terbium in controlling the defect structure, type and concentration of charge carriers, and transport mechanisms in the  $Tb_xSn_{1-x}Se$  system, which is essential for tuning the electronic properties of semiconductors doped with rare-earth elements.

- [1] R. Guo, X. Wang, Y. Kuang, B. Huang. First-principles study of anisotropic thermoelectric transport properties of IV-VI semiconductor compounds SnSe and SnS. *Physical Review B*, 92(11) (2015); DOI:[10.1103/PhysRevB.92.115202](https://doi.org/10.1103/PhysRevB.92.115202)
- [2] S-D. Guo. Thermoelectric properties of orthorhombic group IV-VI monolayers from the first-principles calculations. *Journal of Applied Physics*, 121(3):034302, (2017); DOI:[10.1063/1.4974200](https://doi.org/10.1063/1.4974200)
- [3] A.K. Tolloczko, S.J. Zelewski, J. Ziembicki, et al. Photoemission Study of the Thermoelectric Group IV-VI van der Waals Crystals (GeS, SnS, and SnSe). *ADVANCED OPTICAL MATERIALS*, Vol. 12, Is. 6, 2302049, (2024); <https://doi.org/10.1002/adom.202302049>
- [4] W.R. Shi, M.X. Gao, J.P. Wei, et al. Tin Selenide (SnSe): Growth, Properties, and Applications. *ADVANCED SCIENCE*, 8;5(4):1700602. (2018); doi: [10.1002/advs.201700602](https://doi.org/10.1002/advs.201700602)
- [5] J.I. Huseynov, M.I. Murguzov, S.S. Ismayilov, et al. On the thermopower and thermomagnetic properties of  $Er_xSn_{1-x}Se$  solid solutions. *Semiconductors* 51, 153–157 (2017). <https://doi.org/10.1134/S1063782617020075>
- [6] V. Tayari, B.V. Senkovskiy, D. Rybkovskiy, et al. Quasi-two-dimensional thermoelectricity in SnSe. *Physical Review B*, 97, 045424 (2018); <https://doi.org/10.1103/PhysRevB.97.045424>
- [7] S. Li, Y. Wang, C. Chen, et al. Heavy Doping by Bromine to Improve the Thermoelectric Properties of n-type Polycrystalline SnSe. *ADVANCED SCIENCE*, Vol. 5, Is. 9, 1800598, (2018); <https://doi.org/10.1002/advs.201800598>
- [8] Sh.S. Ismailov, M.A. Musaev, I.I. Abbasov, et al. Effect of doping level and compensation on thermal conductivity in  $Ce_xSn_{1-x}Se$  solid solutions. *Low Temperature Physics*, 46 (11), 1310-1317, (2020); <http://jnas.nbu.gov.ua/article/UJRN-0001168654>
- [9] J.I. Huseynov, M.I. Murguzov, S.S. Ismayilov, Specific features of self-compensation in  $Er_xSn_{1-x}Se$  solid solutions. *Semiconductors* 47, 323–326 (2013). <https://doi.org/10.1134/S106378261303010X>
- [10] I.I. Aliev, J.I. Huseynov, M.I. Murguzov, Sh.S. Ismailov, E.M. Gojaev. Phase relations and properties of alloys in the SnSe-DySe system. *Inorg Mater*, 50, 237–240 (2014). <https://doi.org/10.1134/S0020168514030029>
- [11] Z.G. Liu, J.H. Ouyang, Y. Zhou. Preparation and thermophysical properties of  $(Nd_xGd_{1-x})_2Zr_2O_7$  ceramics. *Journal of Materials Science*, Vol. 43, pp. 3596–3603, (2008); <https://doi.org/10.1007/s10853-008-2570-9>
- [12] D.I. Huseynov, M.I. Murguzov, S.S. Ismailov. Thermal conductivity of  $Er_xSn_{1-x}Se$  ( $x \leq 0.025$ ) solid solutions. *Inorg Mater* 44, 467–469 (2008); <https://doi.org/10.1134/S0020168508050063>
- [13] Y. Huang, C. Wang, X. Chen, et al. First-principles study on intrinsic defects of SnSe. *RSC Advances*, Is. 44, pp. 27139 – 27832, (2017); <https://doi.org/10.1039/C7RA03367B>
- [14] Y. Zhou, W. Li, M. Wu, et al. Influence of defects on the thermoelectricity in SnSe: A comprehensive theoretical study. *Physical Review B*, 97, 245202, (2018); <https://doi.org/10.1103/PhysRevB.97.245202>
- [15] V.Q. Nguyen, T.L. Trinh, C. Chang, et al. Unidentified major p-type source in SnSe: Multivacancies. *NPG Asia Mater* 14, 42 (2022). <https://doi.org/10.1038/s41427-022-00393-5>
- [16] V. Karthikeyan, S.L. Oo, J.U. Surjadi, et al. Defect engineering boosted ultrahigh thermoelectric power conversion efficiency in polycrystalline SnSe. *ACS Applied Materials and Interfaces*, 13(49), pp. 58701-58711. (2021); doi: 10.1021/acsami.1c18194
- [17] J.E. Dill, C.F.C. Chang, D. Jena, H.G. Corre. Two-carrier model-fitting of Hall effect in semiconductors with dual-band occupation: A case study in GaN two-dimensional hole gas. *J. Appl. Phys.* 137, 025702 (2025); <https://doi.org/10.1063/5.0248998>
- [18] I.I. Abbasov, Sh.S. Ismailov, J.I. Huseynov, V.A. Abdurahmanova. Concentration dependences of electrical conductivity and the Hall effect of the  $Ce_xSn_{1-x}Se$  single crystals. *Low Temperature Physics*, 45, 1277–1280 (2019); <https://doi.org/10.1063/10.0000209>
- [19] J.I. Huseynov, T.A. Jafarov. Effect of  $\gamma$ -ray radiation on electrical properties of heat-treated  $Tb_xSn_{1-x}Se$  single crystals. *Semiconductors* 46, 430–432 (2012). <https://doi.org/10.1134/S1063782612040082>
- [20] L-D. Zhao, S-H. Lo, Y. Zhang, et al. Ultralow thermal conductivity and high thermoelectric figure of merit in SnSe crystals. *Nature*, 508(7496):373-7. (2014); doi: 10.1038/nature13184.
- [21] K. Cermak, S. Raitrova, V. Holy, J. Kasparova, et al. As-doped SnSe single crystals: Ambivalent doping and interaction with intrinsic defects. *Physical Review B*, 103, 085203, (2021); <https://doi.org/10.1103/PhysRevB.103.085203>
- [22] H. Liu, S. Zhang, Y. Zhang, et al. Study on the Thermoelectric Properties of n-Type Polycrystalline SnSe by  $CeCl_3$  Doping. *ACS Applied Energy Materials*, 5, 12, 15093–15101, (2022); <https://doi.org/10.1021/acsaem.2c02761>

- [23] *J.I. Huseynov, T.A. Jafarov.* The Influence of  $\gamma$ -Irradiation on Thermoemf and Heat Conduction of  $\text{Ln}_{0.01}\text{Sn}_{0.99}\text{Se}$  (Ln - Pr, Tb, Er) Monocrystals. *World Journal of Condensed Matter Physics*, Vol.4, №.1, p. 1-5, (2014); doi: 10.4236/wjcmp.2014.41001.
- [24] *T. Brumme, M. Calandra, F. Mauri.* First-principles theory of field-effect doping in transition-metal dichalcogenides: Structural properties, electronic structure, Hall coefficient, and electrical conductivity. *Physical Review B* 91, 155436, (2015); DOI:[10.1103/PhysRevB.91.155436](https://doi.org/10.1103/PhysRevB.91.155436)
- [25] *J.I. Huseynov, Kh.A. Hasanov, T.A. Jafarov, I.I. Abbasov.* Compensating effect of terbium impurity on the conductivity of  $\text{Tb}_{1-x}\text{Sn}_x\text{Se}$  solid solutions. *Ukrainian journal of physics*, 65 (3), 225-230, (2020); <http://jnas.nbu.gov.ua/article/UJRN0001127989>

*Received: 02.09.2025*